Templated Synthesis of Carbon Materials from Zeolites (Y, Beta, and ZSM-5) and a Montmorillonite Clay (K10): Physical and Electrochemical Characterization

Curtis J. Meyers,[†] Simit D. Shah,[†] Sejal C. Patel,[†] Rita M. Sneeringer,[†] Carol A. Bessel,*[,†] Norman R. Dollahon,[‡] Randolph A. Leising,*[,§] and Esther S. Takeuchi*[,§]

Department of Chemistry, Villanova University, 800 Lancaster Avenue, Villanova, Pennsylvania 19085, Department of Biology, Villanova University, 800 Lancaster Avenue, Villanova, Pennsylvania 19085, and Wilson Greatbatch Ltd., 10,000 Wehrle Drive, Clarence, New York 14031

Received: August 15, 2000; In Final Form: November 13, 2000

New high surface area carbon materials were prepared at low temperature (600 °C) using zeolite (Y, Beta, and ZSM-5) and montmorillonite clay (K10) templates. Acrylonitrile, furfuryl alcohol, pyrene, and vinyl acetate precursors were polymerized and carbonized in each of the inorganic matrixes without the addition of a polymerizing agent. The templates were removed by acid demineralization and the resulting carbon materials were physically characterized by infrared spectroscopy, BET (N_2) surface area analysis, energy dispersive spectroscopy (EDS), scanning electron microscopy (SEM), and elemental analyses. Electrochemical characterizations were also conducted. Cyclic voltammetry was employed to examine the synthesized carbons in the oxidation of catechol to hydroquinone and quinone, a model reaction that is known to be surface dependent. The identities of both the template and the substrate affected the electrochemical response. Additionally, the ability of the new carbons to intercalate and deintercalate lithium was investigated. While all of the synthesized carbons displayed high irreversible capacities consistent with other low-temperature carbons, the carbons prepared from zeolite Y displayed unique voltage curves, suggesting template effects on the carbon. In addition, all of the carbons prepared for this study displayed significant voltage hysteresis on charge/discharge.

1. Introduction

There has been a recent avalanche of literature focused on the structure-directed or templated synthesis[1−3] of new materials due to the interesting physical, magnetic, and electronic properties that these new materials possess. During templated synthesis methods, substrate or precursor materials are included into the template framework in such a way that their final structure reflects, to differing degrees, the shape of the template. Organic templates are commonly used to synthesize inorganic materials. For example, surfactants have been used to template the synthesis of MCM-41[4] and other porous silicates,[5,6] oxides,[7] sulfates,[8] and layered organic/inorganic composites;[9,10] liquid crystals have been used to template the synthesis of mesoporous silicates or aluminosilicates,[11,12] as well as sulfide and selenide superlattices,[13] and polymer (latex) spheres[14−17] and monodisperse emulsion droplets[18] have been used to template the preparation of metal oxide and carbonate materials. While the preceding represent some of the simpler templating materials, a wide variety of more exotic organic templates, such as self-assembled diblock copolymer films,[19] amines and amine dendrimers,[20−22] carbon nanotubes[23−27] colloids,[28,29] sugar-based lipid tubules,[30] and bacterial superstructures (*Bacillus subtilis*),[31] have also been studied recently. The potential applications of the new materials are important and range from catalysts and catalyst supports to separation materials and membranes, hosts for composite optical materials, biomaterials, quantum electrodes, photocatalysts, battery materials, and thermal, acoustic, and electrical insulators.

Similarly, inorganic templates have been used to synthesize a wide variety of carbon materials. While alumina,[32−34] aluminum oxide,[35−37] and silver nanowires[38] have been used as templates to produce carbon nitride and carbon nanotubes/nanofibers, γ-alumina,[39] silica gel,[40] silica sols,[41,42] silica opal crystals,[43] sintered sodium chloride,[44] layered double hydroxides and other layered structures,[45,46] sepiolite,[5] bentolite L, and other clays[47−54] and zeolites[55−63] have been used as templates to produce porous carbon materials. While efforts have been made to understand and improve the templated synthesis of these latter materials,[64] systematic studies need to be conducted on their controlled synthesis, with the physical characterization of these materials correlated to the electrochemical properties, if new applications of these materials are to come to fruition predictably.

In this article, we describe the use of zeolite and clay templates for the preparation of novel carbon materials. During our template-synthesis method, carbon-containing precursors are incorporated into the organized inorganic matrixes, polymerized, and carbonized. The new carbon materials are collected after acid demineralization of the template matrix. Of the previously used inorganic templates, zeolites are attractive as they are microporous materials with high crystallinity and uniformity of pore size and supercage or channel dimensions.[65−67] Previous studies have examined carbon formation from zeolite Y[57−63] and/or mordenite (MOR),[57,58,63] although other zeolites have been used.[39,55−58,63] Clays also represent an attractive starting

[†]Department of Chemistry, Villanova University. Fax: (610) 519-7167. Internet address: bessel@chem.vill.edu.
[‡] Department of Biology, Villanova University.
[§] Wilson Greatbatch Ltd. Fax: (716) 759-8579. Internet address: rleising@greatbatch.com or etakeuchi@greatbatch.com.

10.1021/jp0029663 CCC: $20.00
Published on Web 02/22/2001

material for templated carbon synthesis because their two-dimensional structures[68] may form layered, graphitelike carbons.[47−54]

This work gives a comparison of carbons synthesized from several zeolites (Y, Beta, and ZSM-5) and montmorillonite clay (K10) templates with different organic precursors [acrylonitrile (acn), furfuryl alcohol (fa), pyrene (pyr), and vinyl acetate (va)]. Unlike other methods for forming template-synthesized carbons, we used a single-step, low-temperature method for the polymerization and carbonization of the organic precursors. This method avoids the need for prepolymerized polymer,[50,51,66] X-ray or γ-ray irradiation,[50,52,54,62] transition metal catalysts,[57−59] or treatments with peroxodisulfate ($S_2O_8^{2-}$) or iodate (IO_3^-).[60,61] Also, the carbons produced by the present method were not heat treated after removal of the templates; thus, this procedure is not expected to result in carbons with extended graphitic structures. These new carbon materials were physically characterized by elemental analyses, energy dispersion spectroscopy (EDS), infrared spectroscopy (FT-IR), scanning electron microscopy (SEM), and BET (N_2) surface area analysis. The surface functionalities of the carbons were probed by electrochemically oxidizing catechol to hydroquinone and quinone, in a model, surface-specific reaction, and then by electrochemically incorporating lithium and examining the resultant charge and discharge profiles.

2. Experimental Procedures

2.1. Sample Preparation. Samples of NaY and montmorillonite clay (K10) were obtained from the Aldrich Chemical Co. Ammonium Beta and ammonium ZSM-5 were donated by Zeolyst International. All clay and zeolite templates were ion-exchanged in 0.1 M NaCl(aq) (20 g of template/L) for 24 h before copiously washing with distilled water and drying at 160 °C overnight. Prior to use, the templates were stored over P_2O_5(s).

2.2. Precursor Incorporation and Carbonization. A 20 g sample of the ion-exchanged template was stirred overnight in 100 mL of acrylonitrile (acn), furfuryl alcohol (fa), or vinyl acetate (va) at room temperature, under N_2(g). The suspension was filtered, washed 4 times with 20 mL of toluene, and dried in air. These precursor-encapsulated samples were carbonized by heating in ceramic boats within a tube furnace at 600 °C under a flow of N_2(g) for 24 h.

As pyrene (pyr) is a solid at room temperature, this precursor was encapsulated into the inorganic templates (20 g) from a 5.6 M solution in toluene (100 mL) which was stirred under N_2(g) overnight. The suspension was filtered, washed with toluene, dried, and carbonized as above.

2.3. Dissolution of Template Framework. The precursor-encapsulated template materials were treated with multiple cycles of concentrated HF, diluted HF (50/50 v/v HF/H_2O), concentrated HCl, diluted HCl (50/50 v/v HCl/H_2O), and copious quantities of water. The resultant, insoluble carbons, denoted templateCprecursor, were filtered, air-dried, and placed under vacuum overnight.

2.4. Physical and Electrochemical Characterization. Carbon and hydrogen analyses were conducted by Atlantic Microlabs, Norcross, GA. The molecular dimensions of the various precursors were calculated by using the Molecular Modeling ProTM: Computational Chemistry Program.[69]

Surface area analyses were performed with an automatic volumetric sorption analyzer (Quantachrome Nova 1200 version 3.50 surface area analyzer) using N_2 as an adsorbate at −196 °C. The surface areas were determined from the BET equation after the samples were vacuum outgassed for 2 h at 125 °C.

FT-IR spectra of the solid samples were obtained from KBr pellets and the neat liquid samples were obtained on NaCl plates using a Perkin-Elmer 1600 series FT-IR spectrophotometer at 4 cm^{-1} resolution. N_2(g) was used to purge the sample compartment.

Energy dispersive spectroscopy (EDS) was performed on a PGT IMIX-XD X-ray analysis system equipped with PGT IMIX MicroAnalysis Software, version 8. The detector was a PGT Omega X-ray detector fitted with a barium light element window. The samples were prepared on carbon adhesive tabs (Electron Microscopy Sciences). Scanning electron microscopy (SEM) was performed on a Hitachi S-570 scanning electron microscope using an accelerating voltage of 15 keV and a working distance of 25 mm. SEM samples were also prepared on carbon adhesive tabs. Scanning electron micrographs were taken with Polaroid Polar Pan 400 film.

Cyclic voltammetry was conducted on an IBM model EC/225 voltammetric analyzer and recorded on a Houston Instruments model 100 $x-y$ recorder. The reference electrode was a saturated sodium chloride calomel electrode (SSCE) and the auxiliary electrode was a Pt wire. The carbon-modified working electrodes were made from glassy carbon electrodes (GCEs, Bioanalytical Systems) modified with a carbon/poly(acrylic acid) coating (PAA, MW_{av} = 750 000) using slight variation of a literature procedure:[70] GCEs were hand polished using 0.3 μm alumina for 30 s, sonicated in distilled water for 30 s, rinsed with fresh distilled water, and then dried. The carbons were lightly ground in a mortar and pestle for 1 min before 10 mg of the ground carbon was added to 1 mL of methanol. Two drops of this mixture were applied to the surface of the GCEs and the methanol was allowed to evaporate. An overcoat of 2 drops of a solution of poly(acrylic acid) (53 mg) in methanol (10 mL) was added to the carbon/electrode surface and the surface was again allowed to dry before use. The electrolyte solutions for cyclic voltammetry studies consisted of either a standard phosphate buffer (pH = 6.78, μ = 0.1) or the standard buffer solution reduced to pH = 2.10 by addition of H_2SO_4. The concentration of catechol was approximately 5 x 10^{-4} M.

Experimental carbon/lithium cells were constructed to examine the ability of the carbon materials to intercalate and deintercalate lithium. These cells consisted of carbon working electrodes, 8.8 x 2.5 cm, with 8% polyvinylidine fluoride (PVDF) binder on copper foil. The working electrodes were prepared by spreading a slurry of the selected carbon and PVDF dissolved in dimethylformamide (DMF) onto copper foil, drying under vacuum at 110 °C, and compacting at 440 kg/cm^2. Lithium foil, 11 x 3.6 cm, was used as the counter electrode, with a nickel tab to make electrical contact. A small lithium metal electrode was also used as a reference electrode. A polyethylene microporous film was used between the working and counter electrodes, and the electrodes were formed into a wound element. The electrolyte was 1 M $LiPF_6$/ethylene carbonate (EC):dimethyl carbonate (DMC) (EC:DMC = 3:7). The water content of the electrolyte was <20 ppm. All experimental cells were assembled and filled under an atmosphere of less than 0.5% humidity. A Bitrode SCN 48-0.5/0.05-5BP battery test system was used in the charge/discharge cycling of the test cells. The cells were charge and discharge tested galvanostatically at 0.01 mA/cm^2, between voltage limits of +1.5 and +0.01 V, at room temperature.

TABLE 1: Structural Characteristics of Zeolite and Clay Templates and the Physical Dimensions of the Organic Precursors

template	typical idealized composition	pore opening,[a] Å	pore vol, $cm^2\ g^{-1}$
NaY[b]	$Na_{56}[Al_{56}Si_{136}O_{384}]\cdot 250H_2O$	7.4−8.0	0.3
Beta[b]	$Na_n[Al_nSi_{64-n}O_{128}]$, $n < 7$	6+	0.2
ZSM-5[b]	$Na_n[Al_nSi_{96-n}O_{192}]\cdot \approx 16H_2O$, $n < 27$	6	0.1
K10[c]	$Si_8(Al_{3.33}Na_{0.67})O_{20}(OH)_4$	9.6[d]	12.5−20[e]

precursor	length,[f] Å	width, Å	depth, Å	max dimen, Å	min dimen, Å
acn	5.98	6.02	3.56	8.15	3.56
fa	8.42	6.44	4.28	12.27	4.07
pyr	11.18	8.73	4.25	11.22	3.74
va	8.47	6.86	4.12	8.98	4.06

[a] For the zeolites Beta, NaY, and ZSM-5, this is the pore size, and for the montmorillonite clay, K10, this is the distance between layers. [b] From refs 65−67. [c] From ref 68. [d] Measured for the dried clay. [e] Under ordinary conditions, one to four monomolecular layers of water separate the clay layers. [f] Length, width, depth, maximum dimension (max dimen), and minimum dimension (min dimen) were calculated by using the Molecular Modeling Pro: Computational Chemistry Program.[69]

TABLE 2: Reaction Yields, Elemental Analyses, H/C Ratios, and Percentage Weight Loss after Heat Treatment

		elemental analyses				
carbon	% yield[a]	% C	% H	% diff[b]	H/C ratio[c]	wt loss,[d] %
NaYCacn	7.8	80.44	3.90	15.66	0.582	13
NaYCfa	47.5	57.61	2.97	39.42	0.619	20
NaYCpyr	19.8	14.72	0.74	84.54	0.603	19
NaYCva	4.2	84.69	2.71	12.60	0.384	14
BetaCacn	4.5	84.92	3.94	11.14	0.557	17
BetaCfa	64.4	88.82	3.21	7.97	0.434	9
BetaCpyr	3.5	86.63	3.47	9.90	0.481	15
BetaCva	7.8	88.86	2.71	8.43	0.366	13
ZSM-5Cacn	0.5	75.93	3.95	20.12	0.624	23
ZSM-5Cfa	27.5	91.87	2.48	5.65	0.324	13
ZSM-5Cpyr	0.5	89.06	4.66	6.28	0.628	86
ZSM-5Cva	3.0	87.08	2.43	10.49	0.335	10
K10Cacn	4.0	87.57	2.22	10.21	0.304	18
K10Cfa	36.3	86.08	3.43	10.49	0.478	9
K10Cpyr	7.3	56.17	2.31	41.52	0.494	23
K10Cva	5.0	74.58	2.88	22.54	0.463	14

[a] % yield = (grams of carbon formed/gram of template initially used to incorporate precursor) x 100%. [b] Diff = 100% − (% C + % H). This difference may be due to the presence of O, Si, Al, F, Cl, or other elements. [c] H/C atomic ratios. [d] Percentage weight of carbon lost after heat treatment under N_2(g) employing a 10 °C/min ramp from room temperature to 600 °C.

3. Results and Discussion

3.1. Carbon Yields and Compositions. Table 1 summarizes the structural characteristics of the zeolite and clay templates as well as the computed physical dimensions of the organic precursors. Table 2 summarizes the reaction yields, elemental analyses, H/C ratios, and percentage weight loss of each carbon material after heat treatment to 600 °C under a nitrogen atmosphere. While the carbon yields from each template/precursor pair are low, they are similar to literature yields for carbons produced from radiation, transition metal catalysts, and other polymer initiators.[50,52,53,57−62]

Notably, the amount of carbon material formed per gram of carbon supplied by the precursor varies widely. On average, the fa precursor produces approximately 8 times more carbon material than va, 12 times more carbon material than acn, and 50 times more carbon material than pyr. This ordering of carbon yield does not follow simple trends in the boiling points of the precursors or in the dimensions of the precursor molecules (Table 1). Simple correlations between the carbon yield and the identity of the template are also not evident. The carbons produced from NaY are, however, the most difficult to purify (requiring several dissolution cycles), and thus, lower yields are obtained from this template due to the increased handling of these carbons during purification.

Finally, the carbon materials reported herein are unique as they are formed without the addition of prepolymerized substrates, chemical initiators, transition metal catalysts, or radiation. We have not directly compared the carbon yields of the template-prepared carbons to carbon materials prepared outside the inorganic matrixes as it has been previously shown that the inorganic templates can impose kinetic and steric constraints on the polymerization[63] and graphitization[59] reactions.

Several factors, other than the identity of the precursor and the template, contribute to the carbon yields. For example, the yield of K10Cfa increased 1.5 times when the dried K10 template is replaced by the "as received" clay (*i.e.*, partially hydrated K10). This increase in yield may result from the increased water content of the untreated clay as the increased water content causes increases in the interlayer spacing and, consequently, more space for the substrate to enter and reside in the inorganic matrix. The concentration of the precursor also affects the carbon yield. In addition to utilizing neat acn, fa, or va, carbons were prepared using 1.0 M solutions of these substrates in toluene. The reactions utilizing the neat substrates result in carbon yields that were more than 6 times greater than those using the more dilute substrate solutions. These results are in agreement with previous studies comparing "melt" and "solvent" preparations in which naphthalene or pyrene were introduced into Bentolite L.[47]

The carbons produced by the current method generally contain 56−90% carbon by combustion analyses. EDS analysis of the resultant carbons indicates the most common impurity is oxygen. Several research groups have attributed the assumed oxygen

content (obtained from the difference in the C/H analyses) to the loss of water,[52,54,63] the loss of other volatile solvent impurities,[47,50,52,53] or the presence of oxygen impurities that may have been introduced into the carbons during the acid treatment.[53,62] Other impurities in our carbons include small amounts of aluminum, sodium, chlorine, or fluorine (remaining from undissolved template or from the demineralization process). These trace metal and nonmetal impurities were not directly quantified by EDS due to their low concentration and the difficulties in finding appropriate standards. The carbons prepared in this study yield H/C ratios of ca. 0.304−0.628, on the higher end of the range found in the literature.[48,51−54,62]

3.2. Infrared Spectroscopy. Each of the newly synthesized carbon materials contains strong, broad stretches at ≈3450−3000 cm^{-1}, which are assigned to a combination of alkene, sp^2 C−H stretches (ca. 3100−3000 cm^{-1}) and O−H stretches (ca. 3400 cm^{-1}).[71] Notably, the observed medium-to-strong C═C absorbances (1560−1640 cm^{-1}) are at lower frequencies than typically expected for C═C (ca. 1600−1660 cm^{-1}), but this is attributed to conjugation effects which also result in the increased intensities of the stretches.[71] The alkene stretching assignment is confirmed by ═C−H out-of-plane (oop) bends between 1000 and 650 cm^{-1}. Several groups of bands attributable to the in-plane C−H bending vibrations of the aromatic rings are also observed: 1240−1310, 1185−1260, and 1115−1180 cm^{-1}. Absorbances in the region 885−835 cm^{-1} are assigned to out-of-plane A_{2u} stretches, while the stretches at *approximately* 1588 cm^{-1} are assigned to the E_{1u} bands of microcrystalline graphite regions which exist within the amorphous carbon materials. These observations are consistent with those of Chen and co-workers.[72]

The infrared spectra of the newly synthesized carbon materials do indicate the presence of impurities. For example, the broad peaks at 3400−3300 cm^{-1} and the peaks at ∼1260 cm^{-1} are typical of hydrogen-bonded O−H stretches (where the alcohol moiety is surface isolated) and the subsequent C−O stretches, respectively. The presence of alcohol moieties may result from oxidation of the active surface groups, especially given the large surface area of the carbons (*vide infra*). Confirming the EDS analysis for the presence of fluorine and chlorine, small absorbances at 1400−1000 cm^{-1} (assigned to C−F stretches) and at 785−540 cm^{-1} (assigned to C−Cl stretches) are also observed.

3.3. Scanning Electron Microscopy. Figure 1 gives typical electron micrographs of the new carbon materials. The micrograph of K10Cacn (Figure 1A) is as expected. The two-dimensional nature of the clay results in soft images of wrinkled thin films that are aggregated to a diameter of approximately 2−6 μm. Unexpectedly, the micrographs of the carbons produced from acn and templates Beta (Figure 1B) and ZSM-5 (Figure 1C) are similar to that of K10Cacn. Unlike the crystalline morphology of the zeolites from which they are synthesized, BetaCacn and ZSM-5Cacn also appear as wrinkled, layered structures with aggregate sizes of *ca.* 6 μm. Since these particle sizes are much greater than the interiors of these inorganic templates, stacking and aggregation during the demineralization and drying process is indicated.[62] Only the micrograph of NaYCacn (Figure 1D) appears as well defined 0.4−0.8 μm particles. This carbon morphology is typical of that which is observed for carbons produced from poly(acrylonitrile) and poly(furfuryl alcohol) after γ-ray irradiation in zeolite Y or from chemical vapor deposition of propylene in zeolite Y.[62]

Notably, our carbon micrographs do not support the conclusion that template-synthesized carbon morphologies depend more on the preparation method than on the identity of the inorganic template.[51,53] We have observed that both the identities of the organic precursors and the templates affect the morphologies of the carbons produced by the template method.

3.4. Surface Area Analyses. The BET surface areas of the inorganic templates and synthesized carbon materials are given in Table 3. The surface areas of the carbons from acrylonitrile range between 458 and 504 $m^2\ g^{-1}$, from furfuryl alcohol between 245 and 636 $m^2\ g^{-1}$, from pyrene from 2.1 to 82 $m^2\ g^{-1}$, and from vinyl acetate from 333 to 947 $m^2\ g^{-1}$. The generally high surface areas of these carbons may result from the kinetics of dehydroxylation, which are faster than the kinetics of carbonization and which may cause the carbons to separate from the template and develop into small microporous particles.[73]

Previously, Sonobe reported surface areas of carbons produced from poly(acrylonitrile) and montmorillionite of only 2 $m^2\ g^{-1}$ prior to post-synthesis heating.[52] Similarly, Sandi and co-workers reported surface areas of 23 $m^2\ g^{-1}$ for carbons prepared from pyrene and Bentolite-L.[48] This surface area was considered high when compared with other carbons that were produced under mild heating (*i.e.*, <1000 °C). While the surface areas reported herein are higher than those from some previous reports, Kyotani and co-workers have determined BET surface areas from 1320 to 2300 $m^2\ g^{-1}$ for the chemical vapor deposition of propylene in zeolite channels.[62]

3.5. Cyclic Voltammetry at Modified Electrodes. Electrochemical investigations using solid carbon electrodes are frequently complicated by effects arising from the variable nature of the electrode surface.[74−77] The composition of the electrode surface is especially important for electrode processes involving concomitant proton and electron transfer. We have investigated the cyclic voltammetry of our template-synthesized carbon materials using a model reaction, the oxidation (and subsequent reduction) of catechol to hydroquinone and quinone. This electrochemical reaction was chosen as it represents a proton/electron transfer process which is known to be highly influenced by the electrode surface and composition.[78−81]

Table 1 and Figure 2 present the cyclic voltammetry data for the carbon-modified electrodes during catechol oxidation and reduction at pH = 2.0. The cyclic voltammetry of the catechol solution at a polished glassy carbon electrode (GCE) is shown in Figure 2A, as a blank. This curve corresponds to catechol oxidation and its associated reduction where the peak potentials are widely separated, the waves are broad, and the peak currents are not equal. This irreversible response has been assigned to a concomitant two electron, two proton process as shown in Figure 3A. In this process, the intermediate oxidation state (hydroquinone) is unstable with respect to disproportionation and the electrode processes are kinetically facile. Figure 2B, shows that the addition of a layer of poly(acrylic acid) causes a slight decrease in the overall peak currents (anodic peak current, $i_{p,a}$, and cathodic peak current, $i_{p,c}$) along with a 20 mV increase in peak current separation (ΔE_p, where $\Delta E_p = E_{p,c}$ (cathodic peak potential) $- E_{p,a}$ (anodic peak potential)). Comparison of these GCE and PAA/GCE electrodes indicates that the PAA binder, used to adhere the new template-synthesized carbon materials to the polished GCE surface, does not significantly effect the electrochemical response of the electrode surface.

Figure 2C−F shows the electrochemical responses when the template remains constant (NaY) but the organic precursors (acn, fa, pyr, and va) are varied. Each of these new carbons results in a distinctive electrochemical response. The NaYCacn- and

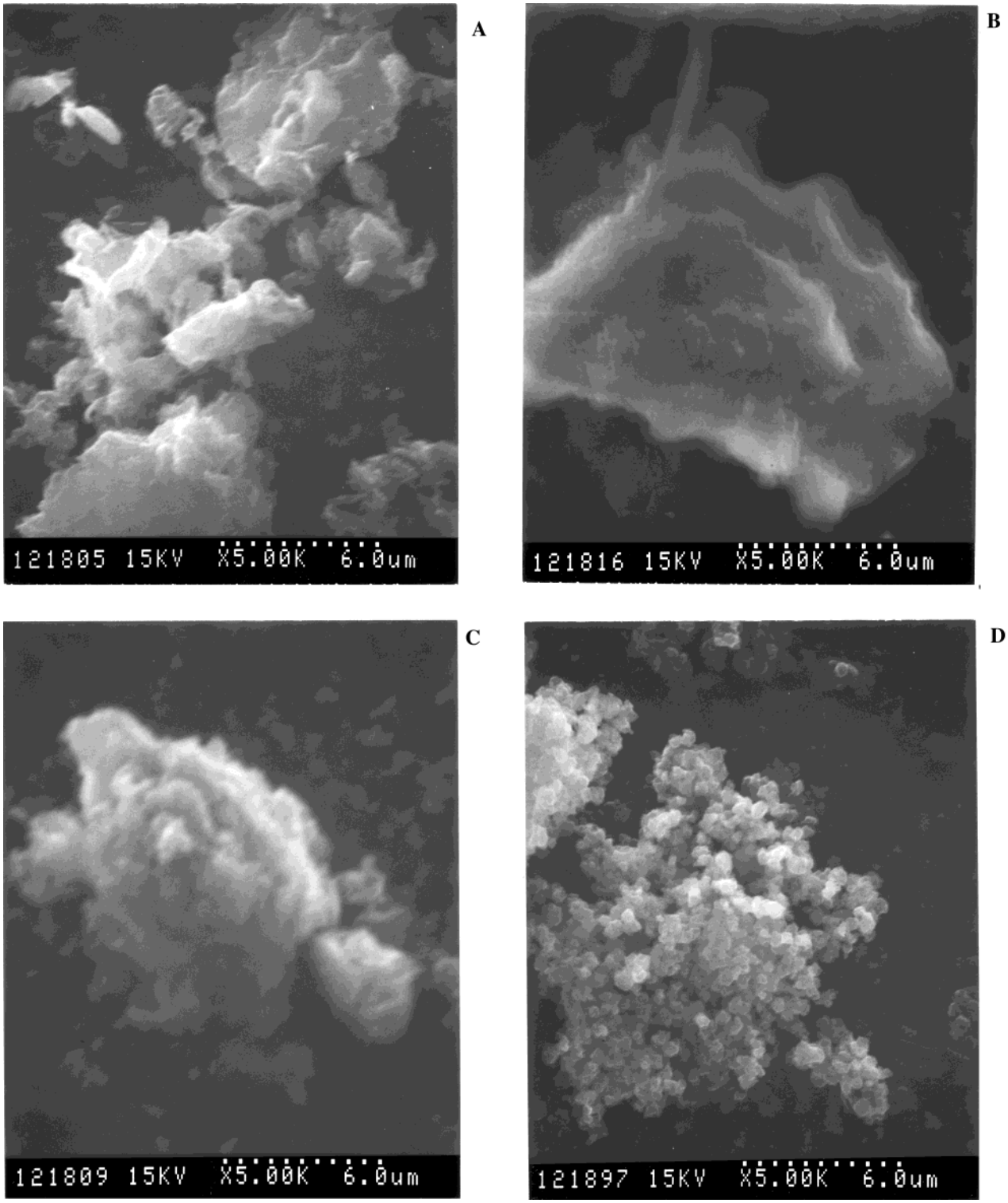

Figure 1. Scanning electron micrographs (SEMs) of carbons synthesized from acrylonitrile: (A) K10Cacn, (B) BetaCacn, (C) ZSM-5Cacn, and (D) NaYCacn. Each micrograph was taken at a magnification of 5000 times.

NaYCpyr-modified electrodes (Figure 2C, E) demonstrate only one set of oxidation and reduction peaks; these have again been assigned to a concomitant two electron, two proton couple (Figure 3A). Notably, while the NaYCpyr-modified electrode demonstrates a response that is similar to the polished GCE alone, the NaYCacn-modified electrode shows an additional catalytic oxidation at +1.0 V. This latter process has not been identified but is probably associated with the catalytic oxidation of NaYCacn surface species. As decreases in ΔE_p values can be used as a qualitative measure for the increase in the heterogeneous charge-transfer rate constant;[82−84] these values (Table 4) indicate the rates follow the order NaYCacn > NaYCpyr > NaYCfa. The electrochemical response of the NaYCfa (Figure 2D) appears as two distinct oxidation and reduction couples, assigned to two distinct one electron, one proton transfers as shown in Figure 3B, C. The second anodic peak, presumably corresponding to the selectively catalyzed process shown in Figure 3C, dominates the first oxidation process.[81] Figure 3F shows that the NaYCva-modified electrode has no electrochemical response toward catechol.

TABLE 3: Surface Area Analyses of Templates and Synthesized Carbon Materials[a]

	template[b]	Cacn	Cfa	Cpyr	Cva
NaY	555	458	422	35	333
Beta	464	468	636	2.2	763
ZSM-5	320	469	245	2.1	947
K10	234	504	627	82	690

[a] All surface areas are in $m^2\ g^{-1}$. All measurements are the average of two or more independent runs. [b]Each template was Na^+ ion-exchanged, dried in an oven at 160 °C for 24 h, and then cooled and stored over P_2O_5(s) for ≥12 h.

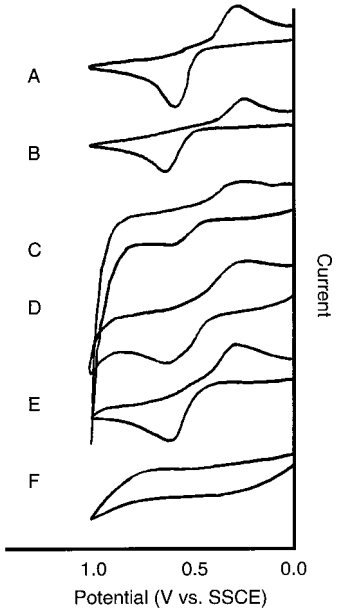

Figure 2. Cyclic voltammetry of 5 x 10^{-4} M catechol in acidified phosphate solution (pH = 2.01, μ = 0.1); Pt auxiliary electrode, saturated sodium chloride reference electrode (SSCE), 100 mV/s, current scales are indicated in parentheses. Working electrode: (A) polished glassy carbon electrode, GCE (2.0 mA/cm); (B) GCE with poly(acrylic acid) coating, PAA/GCE (0.80 mA/cm); (C) NaYCacn/PAA/GCE (0.80 mA/cm); (D) NaYCfa/PAA/GCE (2.0 mA/cm); (E) NaYCpyr/PAA/GCE (2.0 mA/cm); (F) NaYCva/PAA/GCE (40 mA/cm).

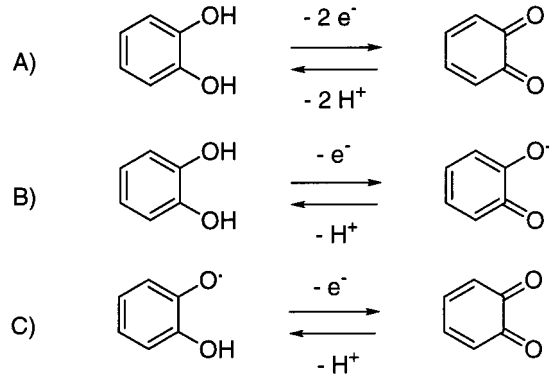

Figure 3. Proposed electrochemical oxidation and reduction processes for catechol.[81]

The oxidation of catechol is expected to show pH dependence in accordance with the Nernst equation;[82] thus we have also examined the electrochemistry of the newly synthesized carbons at pH = 6.78 (Figure 4). At pH = 6.78, NaYCacn, NaYCfa, and NaYCpyr all demonstrate one couple with a wave shape approaching that which is expected for an overall two electron process (Figure 3A). NaYCfa shows the most reversible response, with the smallest ΔE_p (170 mV). The expected 550 mV decrease in redox potential (on going from pH = 2.10 to 6.78 for a two electron process) is much higher than the experimentally observed potential decreases, 298 mV for NaYCacn, 261 mV for NaYCfa, and 157 mV for NaYCpyr, and may reflect the irreversibility of the electrochemical process and electrode materials. Although the catechol electrochemistry can be complicated by adsorption of catechol and/or its oxidation products, the response of the electrode material indicates a solution couple, as the same results were obtained without regard to cycle time or number. Again, the NaYCva-modified electrode showed no (or a highly irreversible) electrochemical response.

Changes in electrochemical response are also observed with the variation of the zeolite or clay template. Figure 5 summarizes the cyclic voltammetry data for catechol oxidation and reduction at electrodes modified with carbons from fa and the various templates. Notably, the response of BetaCfa (Figure 5A) is similar to that of catechol oxidation at an oxidized GC electrode,

TABLE 4: Electrochemical Data for Carbon-Modified Glassy Carbon Working Electrodes

carbon	pH = 2.10[a] $E_{1/2}$ (ΔE_p, V), V	pH = 6.78[a] $E_{1/2}$ (ΔE_p, V), V
GCE alone	0.425 (0.370)	0.186 (0.317)
GCE/PAA	0.435 (0.390)	0.265 (0.640)
BetaCacn	0.450 (0.338)	
BetaCfa	0.444 (0.252)	no response
BetaCpyr	0.415 (0.530)	
BetaCva	0.435 (0.290)	
NaYCacn	0.435 (0.290)	0.137 (0.195)
NaYCfa	0.430 (0.439)	0.169 (0.170)
NaYCpyr	0.440 (0.337)	0.283 (0.307)
NaYCva	no response	no response
ZSM-5Cacn	0.378 (0.401)	
ZSM-5Cfa	0.439 (0.118)	no response
ZSM-5Cpyr	0.440 (0.560)	
ZSM-5Cva	0.475 (0.630)	
K10Cacn	no response	
K10Cfa	no response	no response
K10Cpyr	0.445 (0.350)	
K10Cva	0.437 (0.426)	

[a] Catechol concentration was approximately 5 x 10^{-4} M. SSCE reference, Pt wire auxiliary. Electrolyte: pH = 6.78 standard phosphate buffer, μ = 0.1, or pH = 2.10 solution (*i.e.*, pH = 6.78 standard phosphate buffer was reduced to pH = 2.10 with the addition of H_2SO_4). $E_{1/2} = (E_{p,a} + E_{p,c})/2$.

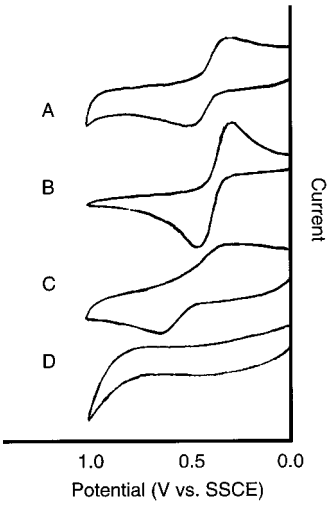

Figure 4. Cyclic voltammetry of 5 x 10^{-4} M catechol in phosphate buffer (pH = 6.78, μ = 0.1); Pt auxiliary electrode, SSCE, 100 mV/s, current scales are indicated in parentheses. Working electrode: (A) NaYCacn/PAA/GCE (0.43 mA/cm); (B) NaYCfa/PAA/GCE (2.1 mA/cm); (C) NaYCpyr/PAA/GCE (2.1 mA/cm); (D) NaYCva/PAA/GCE (8.5 mA/cm).

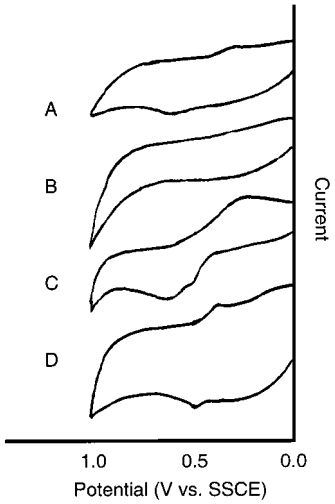

Figure 5. Cyclic voltammetry of 5 x 10^{-4} M catechol in phosphate solution (pH = 2.01, μ = 0.1); Pt auxiliary electrode, SSCE, 100 mV/s, current scales are indicated in parentheses. Working electrode: (A) BetaCfa/PAA/GCE (0.96 mA/cm); (B) K10Cfa/PAA/GCE (9.6 mA/cm); (C) NaYCfa/PAA/GCE (0.96 mA/cm); (D) ZSM-5Cfa/PAA/GCE (2.4 mA/cm).

while NaYCfa (Figures 5C) most resembles the voltammetry which is observed for a catechol solution with a polished electrode.[81] K10Cfa demonstrates no electrochemical response (Figure 3B) while ZSM-5Cfa (Figure 3D) demonstrates the smallest ΔEp of any of the carbons (highest heterogeneous charge-transfer rate constant). The different electrochemical responses of these template-synthesized carbons measured in terms of catechol oxidation indicate that surface properties are not well dominated by either the substrate or template, but by the unique combination of the two. While modeling of the template and substrate parameters may give insight into the physical structures of the newly synthesized materials, the reactivity and potential use of such materials in applications such as catalysts, catalysts supports and electrochemical devices, does not yet appear to be predictable.

3.6. Electrochemical Lithium Intercalation. Experimental carbon/lithium cells were cycle tested to examine the ability of the synthesized carbon materials to store and release lithium ions as a model for carbon anodes used in lithium ion batteries. Data from four carbons prepared from the fa precursor using different templates are given, along with data from four different precursor materials using the same template, NaY. The results of low-rate charge/discharge cycling of the cells are displayed in Table 5. In Table 5, reversible capacity refers to the amount of capacity that can be loaded and unloaded from the carbon material; the irreversible capacity is the amount of capacity displayed during the first charge of the Li/carbon cell which is not returned during the first discharge. The term *charge* here is used to identify the step consisting of the loading of lithium into the carbon, and *discharge* denotes the unloading of lithium from the carbon. This is consistent with the nomenclature for the operation of the carbon anode in a lithium ion battery. The amount of carbon in the sample is calculated based on the electrode weight with the "difference" components (as determined by elemental analyses) subtracted. A commercially available synthetic graphite material, KS-44 from Timcal Inc., is used as a control in the experiment. The total capacity (reversible + irreversible capacity) of KS-44, as measured by our test system, is 435 mA h/g. This is very similar to the total capacity of 445 mA h/g reported for this material in the literature,[85] confirming the accuracy of the experimental setup and measurement. The difference in amount of irreversible capacity, 117 mA h/g reported by Winter and co-workers[85] versus 62 mA h/g found here, may be due to the different electrolyte used in these tests.

The heat treatment temperature of 600 °C used in this study yields disordered carbon materials, consistent with the d_{002} spacing found in the X-ray data for NaYCva (*vide infra*). Compared to the graphite control electrodes, most of the carbons synthesized here give significantly higher reversible capacity during the first discharge cycle. This is consistent with the results for other low temperature, disordered carbons found in the literature.[86−88] Several mechanisms have been proposed to explain this high capacity. Earlier studies have proposed the formation of species such as covalent Li_2 molecules,[89] while more recent work has put forth the "house-of-cards" and "falling-cards" models.[90,91] Wang and Peled have proposed a mechanism for the chemical binding of lithium to the edge carbons in disordered carbon materials to account for the high reversible capacity (600 mAh/g) in these materials.[92,93]

While high reversible capacity is an important goal, these low-temperature carbons also display high irreversible capacity during the first charge step, as seen in Table 5. A substantial part of the irreversible capacity loss which occurs during the first cycle in Li-ion batteries is known to be caused by the reaction of the electrolyte with the carbon anode resulting in a solid electrolyte interface (SEI), or passivation layer, on the carbon surface. Not surprisingly, an increase in the surface area of the carbon anode material can result in an increase in this electrolyte decomposition and a corresponding increase in the irreversible capacity of the system. A correlation between irreversible capacity loss and BET surface area for graphite electrode materials was reported.[85] The BET surface areas for the carbons studied here are in the range 35−640 $m^2\ g^{-1}$, which are quite large, and therefore are expected to result in large irreversible capacities. Irreversible capacity has also been found to depend on the reaction of lithium with surface functional groups on carbon.[91,92] The acid-mediated dissolution of the templates presented here results in the formation of surface functional groups, such as C═O and −OH, as detected by FT-IR analysis, and is also expected to increase the irreversible capacity of the anode. The contribution of these species to the irreversible capacity may be substantial, given that the high surface area of these materials provides many sites for the formation of the functional groups.

On closer examination of the electrochemical data for the individual samples prepared here, some interesting differences are noted. The voltage curves for the first charge step of each of the carbon materials are displayed in Figures 6 and 7. Notably, carbons prepared from the fa precursor all display similar first charge voltage curves, except for NaYCfa. While most of the samples display a voltage plateau at ~1.0 V, the sample prepared from NaY drops smoothly in voltage to ~0.5 V. The appearance of a plateau at 1.0 V during the first charge step is assigned to the reaction of EC solvent with carbon, while reduction of $LiPF_6$ salt on carbon anodes is found at 0.5 V.[94,95] The results here suggest that the unique properties of the carbon resulting from the NaY template may limit the access of EC during the first charge step. This could be due to the nanoscale templating of the carbon by NaY, as suggested by the SEM micrographs of the material. However, the presence of the residual zeolite that was identified in the elemental analyses of this sample must also be considered. The presence of residual zeolite template might block access to some of the pores in the carbon material and limit the reduction of EC during SEI

TABLE 5: Charge/Discharge Cycling Data for Carbon versus Lithium Experimental Cells

carbon	reversible capacity[a] (mAh/g of carbon)	irreversible capacity[b] (mAh/g of carbon)	capacity retention[c] (%)
NaYCacn	274	2935	78
NaYCfa	300	2065	53
NaYCpyr	194	2471	82
NaYCva	391	3710	55
BetaCfa	480	3685	77
ZSM-5Cfa	519	2171	80
K10Cfa	536	2547	67
KS-44d	373	62	90

[a] Reversible capacity = cycle 1 Li-out capacity. [b] Irreversible capacity = cycle 1 Li-in capacity − cycle 1 Li-out capacity. [c]Capacity retention = (cycle 10 Li-out capacity/cycle 1 Li-out capacity) x 100%. [d]KS-44 is a commercially available synthetic graphite used as a control in the experiment.

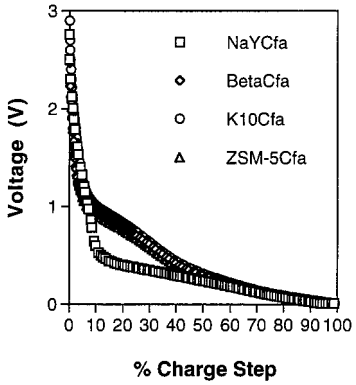

Figure 6. Voltage curves for cycle 1 charge of Li/carbon cells at 0.01 mA/cm^2. Carbons were produced from Beta, Y, ZSM-5 zeolites, and K-10 montmorillonite clay with fa substrate.

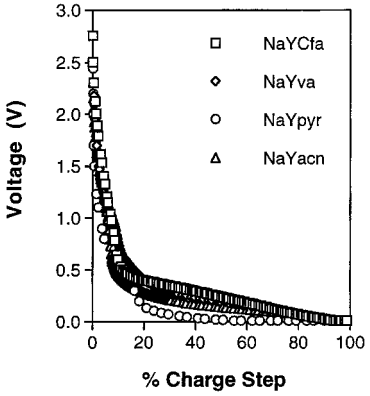

Figure 7. Voltage curves for cycle 1 charge of Li/carbon cells at 0.01 mA/cm^2. Carbons were produced from acn, fa, pyr, and va substrates with zeolite Y.

formation. The voltage curves for the second intercalation of lithium into the carbons prepared from fa are all similar, suggesting that the NaY template has a greater affect on SEI film formation than on reversible lithium intercalation.

The charge and discharge data from carbons produced from the NaY template with different precursors are also presented. As shown in Figure 7, each of the carbon materials displays a different voltage curve during the first charge step. NaYCpyr has a much lower voltage plateau than the other samples. This may be related to the low surface area measured for this sample, which would result in less reactivity at the carbon surface.

Previous studies of low-temperature carbon materials have shown a correlation between the amount of hydrogen contained in the carbon material and the capacity of the system.[96,97] Higher amounts of hydrogen resulted in higher reversible and irreversible capacities. It was proposed that lithium binds on hydrogen-

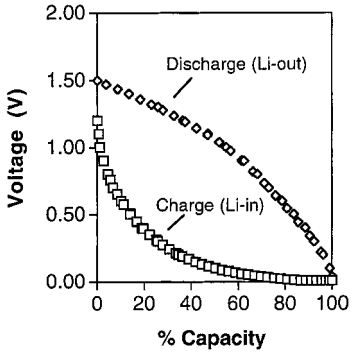

Figure 8. Cycle 2 charge and cycle 3 discharge of Li/NaYCfa test cell at 0.01 mA/cm^2.

terminated edges in the carbon materials in addition to binding between the graphene sheets. Carbons pyrolyzed below 800 °C typically contain high H/C ratios, in the range 0.2−0.4.[97] These high H/C ratio carbons also displayed a large difference in voltage between discharge (near 0 V) and charge (near 1 V). This large hysteresis in potential was attributed to lithium atoms bound near hydrogen atoms.[97] The samples presented here contain high H/C ratios (0.304−0.628) and also display high reversible and irreversible capacity, as well as a large hysteresis, typical of low-temperature carbons. An example of the hysteresis found for the carbons prepared here is illustrated in Figure 8 for the cycle 2 charge and subsequent cycle 3 discharge of a Li/NaYCfa cell. Near the midpoint of the charge/discharge curves, an ∼1 V difference in potential exists for intercalation compared to deintercalation of lithium in these samples.

Capacity retention for the Li/carbon test cells over 10 cycles is listed in Table 5. All of the low-temperature carbon samples tested here give higher capacity fade than the KS-44 graphite control sample. High capacity fade over relatively few cycles, along with the high irreversible capacity found for these samples, severely limits the practicality of these materials for use in Li-ion batteries.

4. Conclusions

We have synthesized new low-temperature carbon materials using combinations of zeolite and montmorillonite clay templates with acrylonitrile, furfuryl alcohol, pyrene, and vinyl acetate precursors. The organic precursors polymerized inside the inorganic templates without the addition of polymerization initiators or metal catalysts. The template-encapsulated precursors were pyrolyzed at 600 °C and the resultant carbons were composed of disordered macrocyclic arrays. The high surface area carbons contained surface alcohols and other oxidation products that were probably introduced during the acid demineralization procedure. The identity of both the inorganic

template and the organic substrate affected the electrochemical response of the carbon-modified electrodes when catechol oxidation and reduction was examined by cyclic voltammetry. On electrochemical incorporation of lithium, all of the carbons displayed high irreversible capacities consistent with other low-temperature carbons; however, the carbons prepared from NaY zeolite displayed unique voltage curves during the first charge step. These results suggest that the NaY zeolite imparts properties on the carbon materials which affect the formation of the SEI layer during lithiation. Finally, while challenges still remain in effectively removing the template materials from the carbon, thus limiting the practicality of this carbon synthesis in lithium ion anode applications, the high surface areas and unique surface compositions may make these carbons interesting catalyst and catalyst support materials.

Acknowledgment. We acknowledge Mr. Brian Scull for his assistance in the infrared spectroscopy experiments, Zeolyst International for a generous donation of ammonium Beta and ammonium ZSM-5, and Mr. Marcus J. Palazzo, Wilson Greatbatch Ltd., for conducting preliminary electrochemical characterizations. This research was accomplished through the generous support of the Office of Naval Research (N00014-96-1-0047, C.A.B.) and Research Corporation (CC4252, C.A.B.).

References and Notes

(1) Martin, C. R. *Chem. Mater.* **1996**, *8*, 1739.
(2) Mann, S.; Ozin, G. A. *Nature* **1996**, *382*, 313.
(3) Hulteen, J. C.; Martin, C. R. *J. Mater. Chem.* **1997**, *7* (7), 1075.
(4) Kresge, C. T.; Leonowicz, M. E.; Roth, W. J.; Vartuli, J. C.; Beck, J. S. *Nature* **1992**, *359*, 710.
(5) Sandi, G.; Carrado, K. A.; Winans, R. E.; Johnson, C. S.; Csencsits, R. *J. Electrochem. Soc.* **1999**, *146* (10), 3644.
(6) Asefa, T.; MacLachlan, M. J.; Coombs, N.; Ozin, G. A. *Nature* **1999**, *402*, 867.
(7) Bagshaw, S. A.; Prouzet, E.; Pinnavaia, T. J. *Science* **1995**, *269*, 1242.
(8) Heywood, B. R.; Mann, S. *J. Am. Chem. Soc.* **1992**, *114*, 4681.
(9) Ukrainczyk, L.; Bellman, R. A.; Anderson, A. B. *J. Phys. Chem. B* **1997**, *101*, 531.
(10) Nguyen, C. V.; Carter, K. R.; Hawker, C. J.; Hedrick, J. L.; Jaffe, R. L.; Miller, R. D.; Remenar, J. F.; Rhee, H.-W.; Rice, P. M.; Toney, M. F.; Trollsas, M.; Yoon, D. Y. *Chem. Mater.* **1999**, *11*, 3080.
(11) Feng, P.; Bu, X.; Pine, D. J. *Langmuir* **2000**, *16*, 5304.
(12) Beck, J. S.; Varuli, J. C.; Roth, W. J.; Leonowicz, M. E.; Kresge, C. T.; Schmitt, K. D.; Chu, C. T.-W.; Olson, D. H.; Sheppard, E. W.; McCullen, S. B.; Higgins, J. B.; Schlenker, J. L. *J. Am. Chem. Soc.* **1992**, *114*, 10834.
(13) Braun, P. V.; Osenar, P.; Tohver, V.; Kennedy, S. B.; Stupp, S. I. *J. Am. Chem. Soc.* **1999,** *121*, 7302.
(14) Holland, B. T.; Blanford, C. F.; Stein, A. *Science* **1998**, *281*, 538.
(15) Holland, B. T.; Blanford, C. F.; Do, T.; Stein, A. *Chem. Mater.* **1999**, *11*, 795.
(16) Caruso, F.; Caruso, R. A.; Mohwald, H. *Chem. Mater.* **1999**, *11*, 3309.
(17) Yan, H.; Blanford, C. F.; Holland, B. T.; Smyrl, W. H.; Stein, A. *Chem. Mater.* **2000**, *12*, 1134.
(18) Imhof, A.; Pine, D. J. *Nature* **1997**, *389*, 948.
(19) Spatz, J. P.; Mossmer, S.; Hartmann, C.; Moller, M.; Herzog, T.; Krieger, M.; Boyen, H.-G.; Ziemann, P.; Kabius, B. *Langmuir* **2000**, *16*, 407.
(20) Larsen, G.; Lotero, E.; Marquez, M. *J. Phys. Chem. B* **2000**, *104*, 4840.
(21) Wang, D.; Yu, R.; Kumada, N.; Kinomura, N. *Chem. Mater.* **2000**, *12*, 956.
(22) Mercier, L.; Pinnavaia, T. J. *Chem. Mater.* **2000**, *12*, 188.
(23) Satishkumar, B. C.; Govindaraj, A.; Vogl, E. M.; Basumallick, L.; Rao, C. N. R. *J. Mater. Res.* **1997**, *12* (3), 604.
(24) Chen, P.; Wu, X.; Lin, J.; Tan, K. L. *J. Phys. Chem. B* **1999**, *103*, 4559.
(25) Ajayan, P. M.; Stephan, O.; Redlich, P.; Colliex, C. *Nature* **1995**, *375*, 564.
(26) Han, W.; Fan, S.; Li, Q.; Hu, Y. *Science* **1997**, *277*, 1287.
(27) Kyotani, T.; Tsai, L.-F.; Tomita, A. *Chem. Commun.* **1997**, 701.
(28) Caruso, F.; Caruso, R. A.; Mohwald, H. *Science* **1998**, *282*, 1111.
(29) Kuther, J.; Seshadri, R.; Nelles, G.; Assenmacher, W.; Butt, H.-J.; Mader, W.; Tremel, W. *Chem. Mater.* **1999**, *11*, 1317.
(30) Archibald, D. D.; Mann, S. *Nature* **1993**, 364, 430.
(31) Davis, S. A.; Burkett, S. L.; Mendelson, N. H.; Mann, S. *Nature* **1997**, *385*, 420.
(32) Sung, S. L.; Tsai, S. H.; Liu, X. W.; Shih, H. C. *J. Mater. Res.* **2000**, *15* (2), 502.
(33) Che, G.; Lakshmi, B. B.; Martin, C. R.; Fisher, E. R. *Langmuir* **1999**, *15*, 750.
(34) Che, G.; Lakshmi, B. B.; Martin, C. R.; Fisher, E. R.; Ruoff, R. S. *Chem. Mater.* **1998**, *10*, 260.
(35) Kyotani, T.; Pradhan, B. K.; Tomita, A. *Bull. Chem. Soc. Jpn.* **1999**, *72*, 1957.
(36) Li, J.; Moskovits, M.; Haslett, T. L. *Chem. Mater.* **1998**, *10*, 1963.
(37) Pradhan, B. K.; Toba, T.; Kyotani, T.; Tomita, A. *Chem. Mater.* **1998**, *10*, 2510.
(38) Liu, S.; Yue, J.; Cai, T.; Anderson, K. L. *J. Colloid Interface Sci.* **2000**, *225*, 254.
(39) Heaviside, J.; Hendra, P. J.; Tsai, P.; Cooney, R. P. *J. Chem. Soc., Faraday Trans. I* **1978**, *74*, 2542.
(40) a) Knox, J. H.; Kaur, B.; Millward, G. R. J. *Chromatography* **1986**, *352*, 3. (b) Gilbert, M. T.; Knox, J. H.; Kaur, B. *Chromatographia* **1982**, *16*, 138.
(41) Han, S.; Hyeon, T. *J. Chem. Soc., Chem. Commun.* **1999**, 1955.
(42) Han, S.; Hyeon, T. *Carbon* **1999**, *37*, 1645.
(43) Zakhidov, A. A.; Baughman, R. H.; Iqbal, Z.; Cui, C.; Khayrulliin, I.; Dantas, S. O.; Marti, J.; Ralchenko, V. G. *Science* **1998**, *282*, 897.
(44) Pekala, R. W.; Hopper, R. W. *J. Mater. Sci.* **1987**, *22*, 1840.
(45) Putyera, K.; Bandosz, T. J.; Jagieo, J.; Schwarz, J. A. *Carbon* **1996**, *34* (12), 1559.
(46) Bandosz, T. J.; Jagiello, J.; Putyera, K.; Schwarz, J. A. *Chem. Mater.* **1996**, *8*, 2023.
(47) Winans, R. E.; Carrado, K. A. *J. Power Sources* **1995**, *54*, 11.
(48) Sandi, G.; Winans, R. E.; Carrado, K. A. *J. Electrochem. Soc.* **1996**, *143* (5), L95.
(49) Sandi, G.; Thiyagarajan, P.; Carrado, K. A.; Winans, R. E. *Chem. Mater.* **1999**, *11*, 235.
(50) Kyotani, T.; Sonobe, N.; Tomita, A. *Nature* **1988**, *331*, 331.
(51) Sonobe, N.; Kyotani, T.; Tomita, A. *Carbon* **1991**, *29* (1), 61.
(52) Sonobe, N.; Kyotani, T.; Tomita, A. *Carbon* **1988**, *26* (4), 573.
(53) Sonobe, N.; Kyotani, T.; Tomita, A. *Carbon* **1990**, *28* (4), 483.
(54) Sonobe, N.; Kyotani, T.; Hishiyama, Y.; Shiraishi, M.; Tomita, A. *J. Phys. Chem.* **1988**, *92*, 7029.
(55) Kyotani, T.; Nagai, T.; Inoue, S.; Tomita, A. *Chem. Mater.* **1997**, *9*, 609.
(56) Rodriguez-Mirasol, J.; Cordero, T.; Radovic, L. R.; Rodriguez, J. J. *Chem. Mater.* **1998**, *10*, 550.
(57) Bein, T. Enzel, P. *J. Chem. Soc., Chem. Commun.* **1989**, 1326.
(58) Bein, T.; Enzel, P. Angew. *Chem. Int., Ed. Engl.* **1989**, *28* (12), 1692.
(59) Enzel, P.; Bein, T. *Chem. Mater.* **1992**, *4*, 819.
(60) Bein, T.; Enzel, P. *Mol. Cryst. Liq. Cryst.* **1990**, *181*, 315.
(61) Enzel, P.; Bein, T. *J. Phys. Chem.* **1989**, *93*, 6270.
(62) Kyotani, T.; Nagai, T.; Inoue, S.; Tomita, A. *Chem. Mater.* **1997**, *9*, 609.
(63) Cox, S. D.; Stucky, G. D. *J. Phys. Chem.* **1991**, *95*, 710.
(64) Lewis, D. W.; Willock, D. J.; Catlow, C. R. A.; Thomas, J. M.; Hutchings, G. J. *Nature* **1996**, *382*, 604 and references therein.
(65) Meier, W. M.; Olson D. H.; Baerlocher, C. *Atlas of Zeolite Structure Types*, 4th ed.; Elsevier: Boston, 1996.
(66) Breck, D. W. *Zeolite Molecular Sieves*, Wiley: New York, 1981.
(67) Smith, J. V. In *Zeolite Chemistry and Catalysis*; Rabo, J. A., Ed.; American Chemical Society: Washington, DC, 1976.
(68) van Olphen, H. *An Introduction to Clay Colloid Chemistry*, 2nd ed.; Wiley: New York, 1977.
(69) Molecular Modeling ProTM: Computational Chemistry Program, Published by WindowChem SoftwareTM Inc., NorGwyn Montgomery SoftwareTM Inc., Fairfield, CA, 1996.
(70) Senaratne, C.; Zhang, J.; Baker, M. D.; Bessel, C. A.; Rolison, D. R. *J. Phys. Chem.* **1996**, *100* (14), 5849.
(71) Pavia, D. A.; Lampman, G. M.; Kriz, G. S. *Introduction to Spectroscopy: A Guide for Students of Organic Chemistry*, 2nd ed.; Harcourt Brace, Philadelphia, 1996.
(72) Wang, Z.; Lu, Z.; Huang, X.; Chen, L. *Carbon* **1998**, *36* (1−2), 51.
(73) Bandosz, T. J.; Putyera, K.; Jagiello, J.; Schwarz, J. A. *Carbon* **1994**, *32*, 659.
(74) Rusling, J. F. *Anal. Chem.* **1984**, *56* (3), 575.
(75) Hoogvliet, J. C.; van den Beld, C. M. B.; van der Poel, C. J.; van Bennekom, W. P. *J. Electroanal. Chem.* **1986**, *201*, 11.
(76) Kamau, G. N. *Anal. Chim. Acta* **1988**, *207*, 1.
(77) Kinoshita, K. *Carbon: Electrochemical and Physicochemical Properties*; John Wiley and Sons: New York, 1988.

(78) Zak, J.; Kuwana, T. *J. Am. Chem. Soc.* **1982**, *104*, 5515.
(79) Zak, J.; Kuwana, T. *J. Electroanal. Chem.* **1983**, *150*, 645.
(80) Aihara, M.; Fukata, M.; Komatsu, M. *Anal. Lett.* **1987**, *20* (5), 669.
(81) (a) Cabaniss, G. E.; Diamantis, A. A.; Linton, R. W.; Murphy, W. R., Jr.; Meyer, T. J. *J. Am. Chem. Soc.* **1985**, *107*, 1845. (b) Murphy, W. R., Jr. Ph.D. Dissertation, The University of North Carolina at Chapel Hill, 1984.
(82) Bard, A. J.; Faulkner, L. R. *Electrochemical Methods*; John Wiley and Sons: New York, 1980; pp 290−91.
(83) The changes are only qualitative, because, in most cases, the ΔE_p values were too large to permit the calculation of the heterogeneous charge-transfer rate constant using the treatment of Nicholson.[84]
(84) Nicholson, R. S. *Anal. Chem.* **1965**, *37*, 1351.
(85) Winter, M.; Novak, P.; Monnier, A. *J. Electrochem. Soc.* **1998**, *145* (2), 428.
(86) Mabuchi, A.; Tokumitsu, K.; Fujimoto, H.; Kasuh, T. *J. Electrochem. Soc.* **1995**, *142* (4), 1041.
(87) Deschamps, M.; Yazami, R. *J. Power Sources* **1997**, *68*, 236.
(88) Liu, Y.; Jue, J. S.; Zheng, T.; Dahn, J. R. *Carbon* **1996**, *34* (2), 193.
(89) Sato, K.; Noguchi, M.; Demachi, A.; Oki, N.; Endo, M. *Science* **1994**, *264*, 556. Zheng, T.; Xue, J. S.; Dahn, J. R. *Chem. Mater*. **1996**, *8* (2), 389.
(90) Dahn, J. R.; Zheng, T.; Liu, Y.; Xue. J. S. *Science* **1995**, *270*, 590.
(91) Xing, W.; Dahn, J. R. *J. Electrochem. Soc.* **1997**, *144*, 1195.
(92) Matsumura, Y.; Wang, S.; Mondori, J. *J. Electrochem. Soc.* **1995**, *142*, 2914.
(93) Peled, E.; Eshkenazi, V.; Rosenberg, Y. *J. Power Sources* **1998**, *76*, 153.
(94) Ogumi, Z.; Inaba, M. *Bull. Chem. Soc. Jpn.* **1998**, *71*, 521.
(95) Takeuchi, E. S.; Rubino, R. *J. Power Sources* **1999**, *81−82*, 373.
(96) Zheng, T.; Liu, Y.; Fuller, E. W.; Tseng, S.; von Sacken, U.; Dahn, J. R. *J. Electrochem. Soc*. **1995**, *142* (8), 2581.
(97) Zheng, T.; Xue, J. S.; Dahn, J. R. *Chem. Mater*. **1996**, *8* (2), 389.